Pt nanoparticles decorated TiO_2 nanotubes for the reduction of olefins

V. C Anitha, [a] Anandarup Goswami,[b] Hanna Sopha,[a] Devaki Nandan,[b] Manoj B. Gawande[b]
Klara Cepe, [b] Siowwoon Ng,[a] Radek Zboril[b], Jan M. Macak*[a]

[a]Center of Materials and Nanotechnologies, Faculty of Chemical Technology, University of Pardubice, Nam. Cs. Legii 565, 53002 Pardubice, Czech Republic.

[b]Regional Centre of Advanced Technologies and Materials, Department of Physical Chemistry, Faculty of Science, Palacky University, Slechtitelu 27, 783 71 Olomouc, Czech Republic.

*Corresponding author: Tel: +420 466037 401

E-mail: jan.macak@upce.cz (J.M. Macak)

Abstract

High surface area TiO_2 nanotubes (TNTs) were used as a catalyst support for well dispersed, stable and ultra-small (3-5 nm) Pt nanoparticles (Pt@TNTs) for the reduction of olefins. Pt@TNT catalyst was synthesized by a simple soaking of anodized TNTs in the chloroplatinic (H_2PtCl_6) acid solution. Various techniques such as XRD, SEM, TEM, and XPS were used to characterize the materials and its catalytic property for the olefin reduction has been described along with a proposed mechanism. The Pt@TNT catalyst showed moderate to high catalytic conversions of styrene and its derivative to ethyl benzene-based products using hydrazine hydrate as a reducing agent. An excellent catalytic activity along with high product selectivity was achieved using low amount (10 mg) of Pt@TNT catalyst containing ~2.2 wt.% Pt and short reaction time (45 minutes).

Keywords: TiO_2 nanotubes, Anodization, Pt nanoparticles, Catalysis, Reduction of Olefins

1. Introduction

Advanced nanomaterials are playing important and significant role in current technologies because of their unique physicochemical properties and large-scale applicability in various fields including, nanoelectronics, catalysis, sensors, photonics, biomaterials and biomedicine [1,2]. Based on desirable characteristics, such as surface area, chemical composition, stability and mechanical properties, several nanomaterials such as alumina, zeolites, carbon nanofibers/nanotubes, active carbon and metal oxides have been used as catalysts/support in the past for various applications [3-7].

Among numerous catalysts, Pt nanoparticles supported mainly by carbon based materials, represent proven catalysts for many reactions for example in fuel cells [8,9], for partial hydrogenation/hydrogenation of nitrobenzene [10,11], oxygen reduction reaction [12] and photocatalytic hydrogen generation [13]. Although carbon based materials are broadly established as support materials, the loss of catalytic activity and poor surface stability are their shortcomings [14]. In addition, many catalytic systems suffer from high nanoparticle loading or low catalytic activities due to the nanoparticle agglomeration and catalyst deactivation [15]. Therefore, developing a non-carbon based support material with high specific surface area and stability, with well-dispersed nanoparticles is demanded for an efficient catalyst to enhance the performance largely. Among potentially interesting supports to be used in catalysis, anodic TiO_2 nanotubes (TNTs) are of particular significance due to their superior specific surface area, favorable surface chemistry, stability in acid or alkaline media, efficient loading of the catalyst due to the hollow structure [16,17]. These nanotube layers have shown to be promising for many applications in the fields of photocatalysis [18,19], supercapacitors [20,21], various solar cells [22-26] and biomedicine [27-30]. The advantage of using high surface area TiO_2 nanotubes as a catalyst support is that spreading the active catalytic Pt nanoparticles on walls of TNT results in

good distribution of catalytic Pt nanoparticles throughout the nanotubular structure, leading to a large active catalytic surface per unit weight.

Among industrial catalytically assisted reactions, the hydrogenation of unsaturated hydrocarbons is one of the most widely used methods for the synthesis of saturated hydrocarbons [31,32]. It is generally carried out with transition metal based catalyst (Ni, Pd, Pt, Rh) and hydrogen as a reducing agent [31-36]. One of the drawbacks of these conventional catalytic methods is the use of flammable hydrogen gas at high pressure and elevated temperatures. In that context, in comparison to other liquid hydrogen donors such as ethanol, formic acid, propanol, ammonium formate etc. [37-42], the use of hydrazine hydrate for the reduction of olefins is emerging as one of the best approaches for the liquid phase catalytic hydrogenations in both academia and industry, as it facilitates easy/safer handling of chemicals and avoids complications related with the reactor's design. Moreover, it produces only environmentally benign nitrogen and water as byproducts [32, 43-50].

Several methods are described in the literature for Pt catalysts deposition on TNTs that have various dimensions/morphologies and focus on various catalytic and sensing applications [51-56]. However, to the best of the authors´ knowledge, all previous papers report on uniform Pt nanoparticle´s decoration of only low aspect ratio TiO_2 nanotubes (given the thickness of the tube layers divided by the diameter, the maximum value being reported as 39 in ref. [51]). Here, we report the synthesis of a catalyst consisting of comparably higher aspect ratio TiO_2 nanotube layers (≈ 136) and resulting high surface area as a support for Pt nanoparticles (3-5 nm) and the catalytic performance of Pt@TNT catalyst, used for the first time for the reduction of alkenes to corresponding saturated hydrocarbons using hydrazine hydrate as a reducing agent.

2. Experimental

2.1 Synthesis of anodic TiO_2 nanotube layers

TiO_2 nanotube layers with a thickness of ~15 μm and an inner nanotube diameter of ~110 nm were prepared by anodization of Ti foils (Sigma-Aldrich, 0.127 mm thick, 99.7% purity) at 60 V for 4 h (the sweep rate was 1 V/s), as published previously [57]. These conditions were selected because they yield a reproducible synthesis of high aspect ratio nanotube layers, which were very suitable for the catalytic study conducted in this work. Ti foils were degreased by sonication in isopropanol and acetone prior anodization, then rinsed with isopropanol and dried in air. The anodization was carried out at room temperature in an ethylene glycol electrolyte containing 170 mM NH_4F (Sigma-Aldrich, reagent grade) and 1.5 vol% deionized water. Before the first use, the electrolyte was aged for 9 h (for details, see ref. [57]. The electrochemical setup consisted of a high voltage potentiostat (PGU-200V, Elektroniklabor GmbH) in a two-electrode configuration, with a Pt foil as the counter electrode and a Ti foil as the working electrode. After anodization, the Ti foils were rinsed, sonicated in isopropanol and dried in air.

2.2 Synthesis of Pt@TNT

Pt nanoparticles were loaded within to TiO_2 nanotubes by a simple soaking method; nanotubes grown on Ti foils were soaked in 0.01 mol/g chloroplatinic acid (H_2PtCl_6, Safina Ltd.) solution (water:isopropanol 50:50 vol%) for 1 h, provided that the solution with nanotubes was sonicated for first and last 3 minutes. Afterwards, layers were removed from the solution, left to naturally dry, and air annealed at 300 °C for 1 h in a muffle oven using 4.7 °C/min heating rate. This annealing step led to the thermal decomposition of chloroplatinic acid (H_2PtCl_6) yielding metallic Pt nanoparticles. After the annealing process, TiO_2 nanotubes and Pt loaded TiO_2 nanotubes (Pt@TNT) were separated out from Ti foil by a mechanical bending method. This led

to the fracture of layers into bundles of nanotubes. Based on the gravimetrical comparison of Pt-loaded and blank TiO_2 nanotubes, the Pt loading of ~2.2 wt.% within TiO_2 nanotubes was obtained. The overall catalyst preparation is schematically represented in Fig. 1 and it includes the synthesis of high surface area TiO_2 nanotubes by anodization, Pt nanoparticles loading on nanotubes and separation of Pt@TNTs catalyst from Ti foils.

Fig. 1: Schematic representation of TiO_2 nanotube synthesis, Pt loading on nanotubes and separation of Pt@TNT catalyst.

2.3 Characterization of Pt@TNT catalyst

The morphology of TiO_2 nanotubes and Pt@TNTs was characterized by a field emission scanning electron microscope (FE-SEM, JEOL JSM 7500F) and a high-resolution transmission electron microscope (HR-TEM, TITAN 300, FEI). The cross-sectional views were obtained from fractured samples subjected to mechanical bending.

Fig. S1 shows a representative cross-sectional SEM image of a nanotube layer with thickness of ≈ 15 μm. Grazing Incidence X-ray Diffraction (GIXRD) patterns of the TiO_2 nanotubes and Pt@TNT samples were collected using an Empyrean diffractometer (PANalytical) equipped with a 3-axis cradle and a multichannel detector (PIXcel 3D), Co-Kα radiation (40 kV, 40 mA, λ = 0.1789 nm), for the analyzed samples, the incidence angle ω = 0.5°. XPS surface investigation has been performed on the PHI 5000 VersaProbe II XPS system (Physical Electronics) with monochromatic Al-Kα source (15 kV, 50 W); photon energy of 1486.7 eV was employed. Dual beam charge compensation was used for all measurements. All the spectra were measured in the vacuum (1.3×10^{-7} Pa) and at the room temperature (21 °C). The analyzed area on each sample was a spot of 200 μm in diameter. The survey spectra was measured with pass energy of 187.850 eV and electronvolt step of 0.8 eV while for the high resolution spectra was used pass energy of 23.500 eV and electronvolt step of 0.2 eV. The spectra were evaluated with the MultiPak (Ulvac - PHI, Inc.) software.

2.4 Catalytic Reduction of Olefins

In a 10 mL vial, equipped with magnetic stirrer, 0.1 mmol substrate (styrene, 4-methyl styrene and 4-fluro styrene, Sigma-Aldrich), 10 mg Pt@TNT catalyst, and 0.5 mL ethanol (EtOH, Sigma-Aldrich) were taken to which 50-μL hydrazine hydrate ($N_2H_4.H_2O$, Sigma-Aldrich) as a reducing agent was added. The reaction was carried out under microwave irradiation (MW, 850 W) at 90 °C for 45 minutes. Furthermore, the catalytic efficiency of the Pt@TNT was compared with that of commercially available Pt black (Sigma-Aldrich), TNT, physical mixture of Pt black and TNT, using the same weight ratio of Pt nanoparticles under optimized reaction conditions. On completion of the reaction, the contents were diluted with ethanol, the catalyst was filtered and crude reaction mixture was analyzed using gas

chromatography (GC, Agilent 6820) with an Agilent DB-5 capillary column (30 m x 0.32 mm, 0.5 m) under the operation parameters.

3. Results and Discussion

Fig. 2a and 2b show SEM images of blank TiO_2 nanotubes and Pt nanoparticles decorated TiO_2 nanotubes (Pt@TNTs), respectively. The average inner tube diameter and tube wall thickness are ~110 nm and ~15 nm, respectively. The morphology and homogenous distribution of Pt nanoparticles were confirmed by TEM images shown in Fig. 2c and 2d. The insets of Fig. 2c and 2d show the higher magnification images revealing very narrow dispersion of nanoparticles diameters in the range of 3 to 5 nm. Additional higher magnification top view and cross-sectional SEM images are shown in Fig. S2.

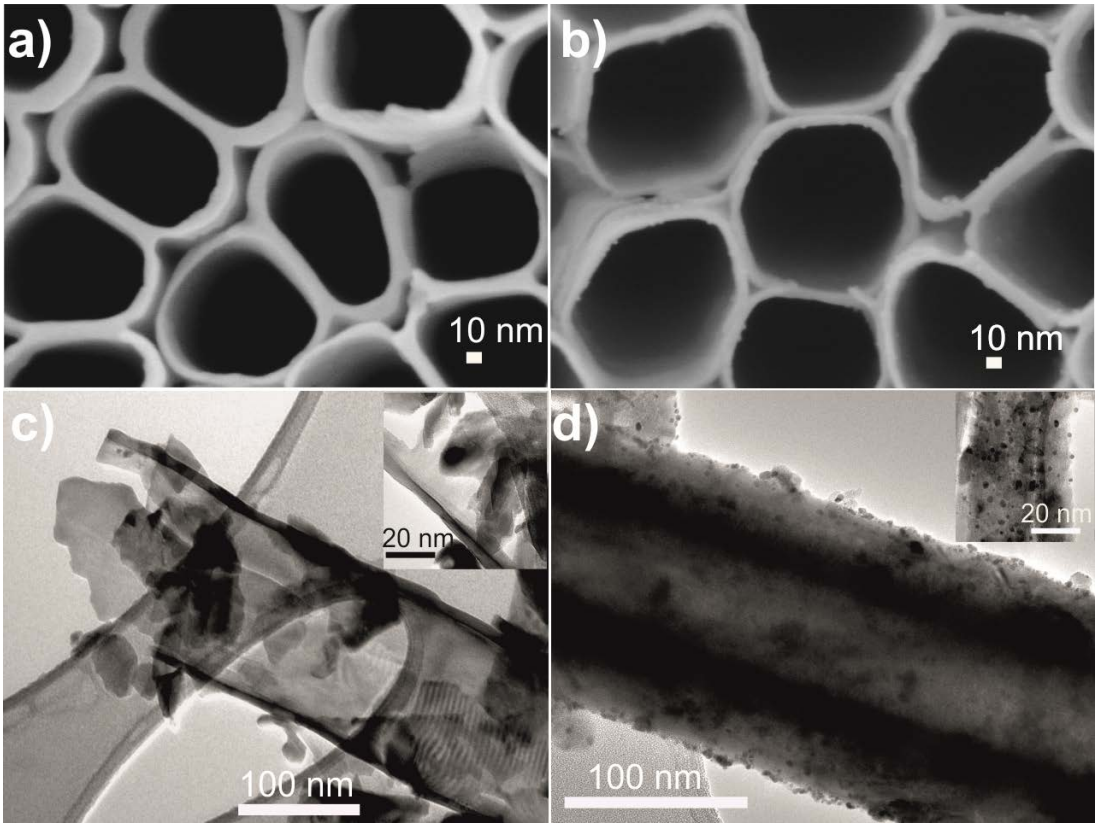

Fig. 2: FE-SEM images of (a) TiO_2 nanotubes, (b) Pt decorated TiO_2 nanotubes, corresponding HR-TEM images are shown in (c) and (d). Insets represent the higher magnification images respectively.

Moreover, successful loading of Pt nanoparticles on the TiO_2 nanotubes was further demonstrated using TEM elemental mapping. Fig. 3 shows that a bright field TEM image of a fragment of Pt@TNT and the elemental mapping (Ti, O, and Pt). It reveals that Pt nanoparticles are well dispersed on the TiO_2 nanotubes, which is crucial for the catalytic activity.

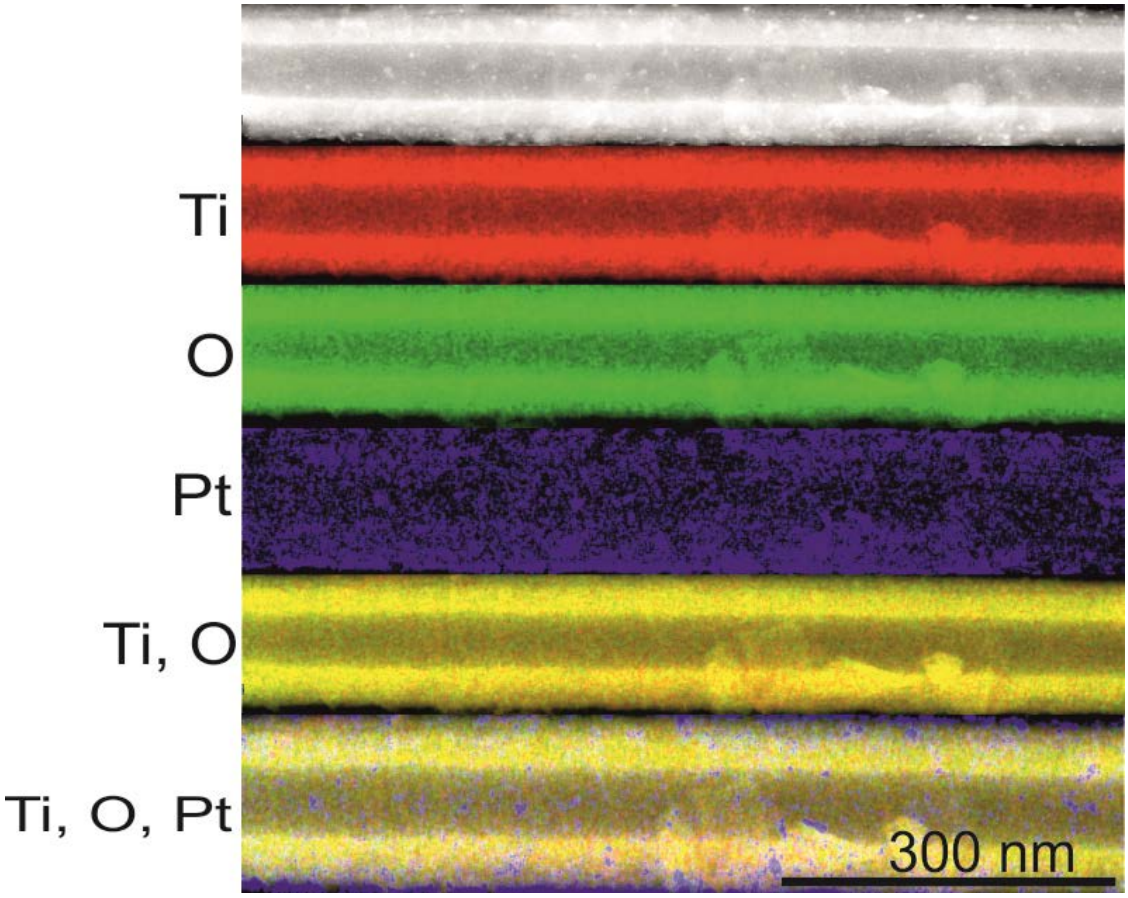

Fig. 3: TEM bright field image and elemental mapping of a fragment of Pt@TNT sample.

Fig. 4a shows the X-ray diffraction (XRD) patterns of blank TiO_2 nanotube layers and Pt decorated TiO_2 nanotube layers (Pt@TNT), respectively. In both patterns, peaks of anatase TiO_2

nanotube layer and of metallic Ti (coming from the substrate underneath the nanotube layer) are clearly identified. The XRD pattern of nanotube layer decorated with Pt nanoparticles showed diffraction peaks at 2Θ=45.9° (111), 2Θ=53.5° (200), 2Θ=79.5° (220) corresponding to the planes of metallic Pt in the cubic lattice (matching with JCPDS PDF #01-087-0636), respectively, clearly confirming the presence of metallic Pt within TiO_2 nanotube layers. The oxidation state of Pt was further analysed by XPS spectra as shown in Fig. 4b. Deconvolution of XPS spectrum in the Pt4f region identified the presence of doublet (7/2-5/2) having binding energy (B.E.) of 70.54 eV (Pt $4f_{7/2}$) and 73.89 eV (Pt $4f_{5/2}$), clearly confirming the presence of Pt(0) [58,59]. The deconvoluted XPS spectrum of Ti2P (Fig. 4c) with the doublet (3/2-1/2) having binding energy (B.E.) of 458.73 eV (Ti $2P_{3/2}$) and 464.57 eV (Ti $2P_{1/2}$) corresponds to the characteristics of the Ti(IV) [60].

The well-synthesized and characterized Pt@TNT employed for the catalytic conversions of styrene using hydrazine hydrate as a reducing agent, compared with additional different catalysts: Pt@TNT, blank TiO_2 nanotubes, Pt black, physical mixture of Pt black and TNT (using the same weight amount of Pt nanoparticles - 2.2 wt.%) under optimized reaction conditions as shown in Fig. 5. There was no appreciable reaction in the absence of any catalyst. The fact that the Pt@TNT yielded highest conversion efficiencies than the physical mixture of the individual counterparts clearly demonstrated the active synergism of the different components of the catalysts. We believe that the synergism comes from the facile activation of hydrazine to yield “active” hydride species, possibly due to better charge transport achieved at the heterojunction between Pt nanoparticles and TNT. Due to different Fermi levels of TNTs and Pt nanoparticles, a Schottky barrier can be formed in the Pt@TNTs. Consequently, there is a refinement of the charge carrier transfer where the energetic difference at the semiconductor

TNT/metallic Pt nanoparticle interface drives electrons from the conduction band of the TNT into the metallic Pt nanoparticles.

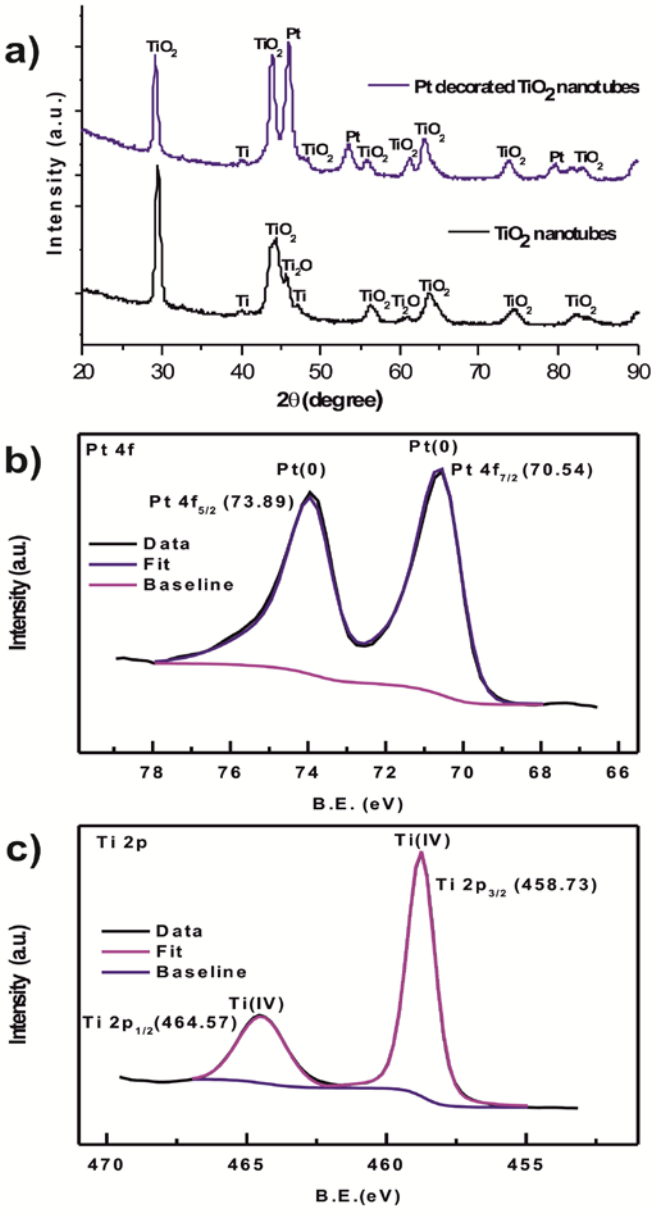

Fig. 4: (a) XRD patterns of blank TiO_2 nanotubes and TiO_2 nanotubes decorated with Pt nanoparticles (Pt@TNT). Deconvoluted XPS spectra of the Pt@TNT catalyst in the regions of (b) Pt 4f and (c) Ti 2p.

Further, the metallic Pt acts as an electron trap, minimizing recombination of the electron-hole pairs and promoting interfacial charge transfer. Such synergism was already demonstrated in the literature and was used for more efficient photocatalytic decomposition of model dyes compared to the uncoated nanotube counterparts [19]. Noteworthy is also the influence of a high number of catalytically active sites (Pt nanoparticles) [61] on 1D-nanotube walls that offer high surface area and great diffusion of reactants/products/intermediates within nanotubes in the same time. Such synergism and high number of catalytic sites cannot be achieved by conventional catalyst carriers with lower specific area and unsuitable dimensionality. Under the optimization reaction conditions used in Fig. 5a, three different types of styrene were catalytically reduced. The catalytic conversions are shown in Fig. 5b.

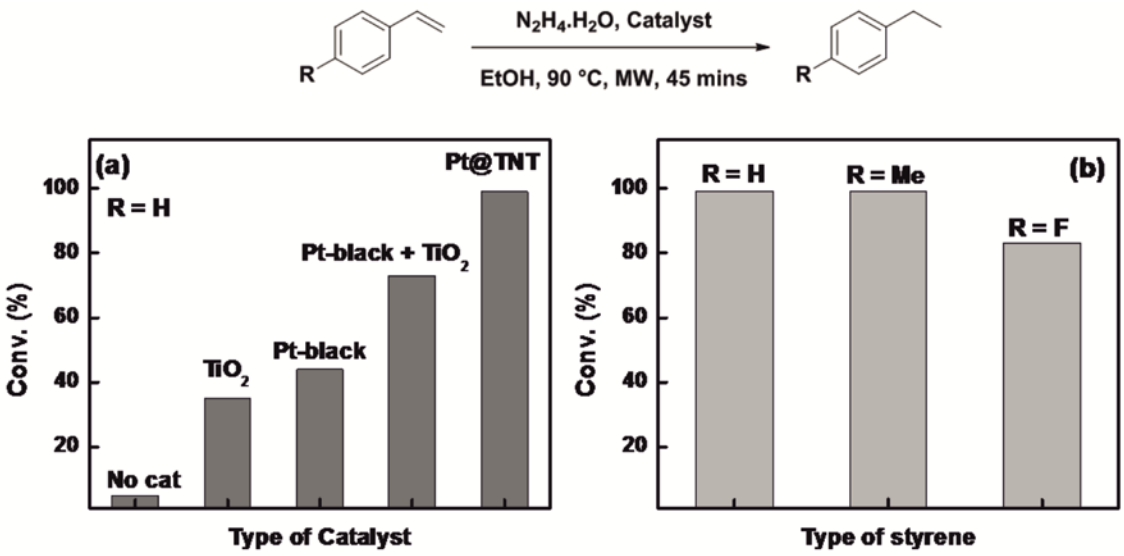

Fig. 5: (a) Conversion efficiencies of styrene with different catalysts and (b) Conversion efficiencies of different styrene derivatives using Pt@TNT. Reaction Conditions: 0.1 mmol of olefin, 0.5 mL of ethanol, $N_2H_4.H_2O$ (50 μL), 10 mg of catalysts (except "no cat" entry), time 45 minutes, temp. 90 ^oC. Conversions were calculated based on GC analyses.

Notably, 4-methyl styrene and 4-fluoro styrene worked well to obtain corresponding products namely 4-methyl ethyl benzene and 4-fluoro ethyl benzene in 99% and 83% conversions (~ 22% defluorinated product) respectively. The reasons for slightly lower conversion efficiency of fluorinated styrenes can be due to electron withdrawing effect of fluorine. As far as the mechanism (and possible synergism) is concerned, in Pt@TNT catalyst, we believe that, the initial formation of titanium-hydride complex (**III**) allows overcoming the initial kinetic barrier of Pt-hydride formation as shown in Fig. 6. Next, the facile hydride transfer at the interface of Pt and TiO_2 provides a unique opportunity to the nanocatalysts to generate the Pt-hydride complex (**V**), which undergoes subsequent reactions (via intermediates **VI** and **VII**) to form the desired product.

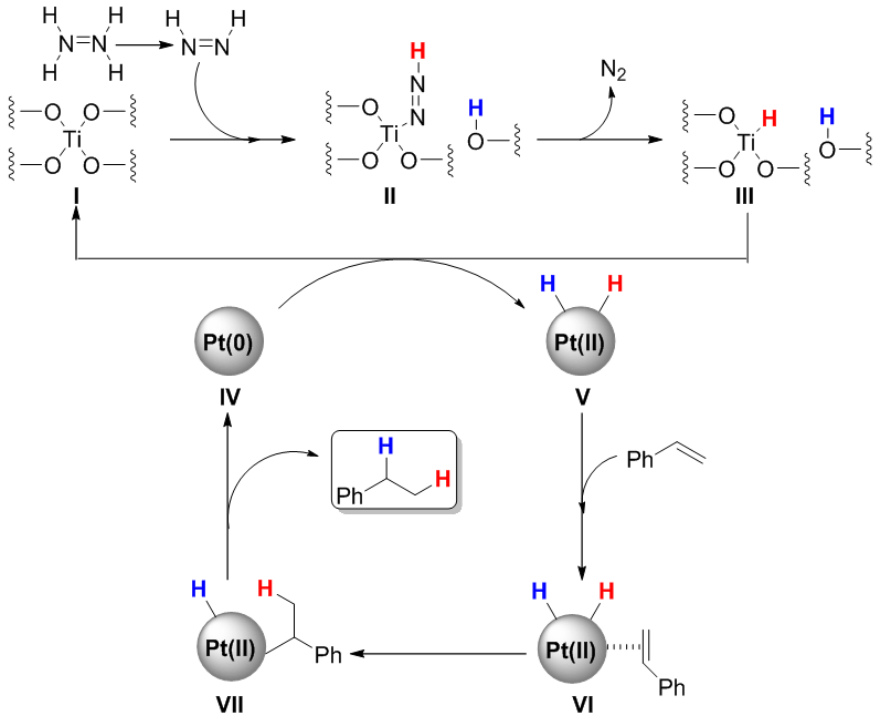

Fig. 6. Plausible mechanism on Pt@TNT nanocatalyst (Formation of titanium-hydride complex, facile hydride transfer at the Pt-TiO_2 interface, generation of Pt-hydride complex).

4. Conclusions

High surface area TiO_2 nanotube layers synthesized by anodization were used as a catalyst support for well-dispersed Pt nanoparticles and applied for catalytic hydrogenation of olefins. Pt@TNTs showed best results (>99% conversion of styrene to ethylbenzene) in comparison to other relevant catalysts, which clearly demonstrated the active synergism of the individual components of the catalysts. The presented Pt@TNT catalyst offers high flow rates and great diffusion of reaction species throughout the nanotubes, and increasing the catalytic activity. The synergetic effect of TiO_2 nanotube layers and decorated Pt nanoparticles can give rise to profound enhancement of the catalytic activities for many other reactions, which relies on the use

of Pt catalyst. Utilization of well-dispersed and small size Pt particles on a high surface area could make the catalysis more efficient in terms of costs and yields.

Acknowledgements

The authors gratefully acknowledge support from the European Research Council (ERC, project No. 638857) and the Ministry of Education, Youth and Sports of the Czech Republic (projects LO1305). The authors also acknowledge the assistance provided by the Research Infrastructures CEMNAT and NanoEnviCz, supported by the Ministry of Education, Youth and Sports of the Czech Republic under projects LM2015082 and LM2015073, respectively. We thank Dr. Veronika Podzemna and Mrs. Denisa Janebova for SEM imaging and technical help with sample preparations. Author also thanks to M. Petr for XPS, Dr. C. Aparicio for XRD analysis.

References

[1] C. Sanchez, P. Belleville, M. Popalld, L. Nicolea, Applications of advanced hybrid organic-inorganic nanomaterials: from laboratory to market, Chem. Soc. Rev. 40 **(**2011) 696-753.

[2] Z. Zhang, B. Xu, X. Wang, Engineering nanointerfaces for nanocatalysis, Chem. Soc. Rev. 43 (2014) 7870-7886.

[3] R. K. Sharma, S. Sharma, S. Dutta, R. Zboril, M.B. Gawande, Silica-nanosphere-based organic–inorganic hybrid nanomaterials: synthesis, functionalization and applications in catalysis, Green Chem. 17 **(**2015) 3207-3230.

[4] X. Wang, Z. Li, J. Shi and Y. Yu, One-Dimensional Titanium Dioxide Nanomaterials: Nanowires, Nanorods, and Nanobelts, Chem. Rev. 114 **(**2014) 9346-9384.

[5] S. Rouhi, Y. Alizadeh, R. Ansari, On the interfacial characteristics of polyethylene/single-walled carbon nanotubes using molecular dynamics simulations, Appl. Surf. Sci. 292 (2014) 958-970.

[6] R. Ansari, S. Ajori, S. Rouhi, Structural and elastic properties and stability characteristics of oxygenated carbon nanotubes under physical adsorption of polymers, Appl. Surf. Sci. 332 (2015) 640-647.

[7] R. Ansari, S. Rouhi, S. Ajori, On the Interfacial Properties of Polymers/Functionalized Single-Walled Carbon Nanotubes, Braz. J. Phys. 46 (2016) 361-369.

[8] Y. H. Lin, X. L. Cui, C. Yen, C. M. Wai, Platinum/carbon nanotube nanocomposite synthesized in supercritical fluid as electrocatalysts for low-temperature fuel cells, J. Phys. Chem. B 109 **(**2005) 14410-14415.

[9] Y. Y. Mu, H. P. Liang, J. S. Hu, L. Jiang, L. J. Wan, Controllable Pt nanoparticle deposition on carbon nanotubes as an anode catalyst for direct methanol fuel cells, J. Phys. Chem. B 109 **(**2005) 22212-22216.

[10] V. Lordi, N. Yao, J. Wei, Method for supporting platinum on single-walled carbon nanotubes for a selective hydrogenation catalyst, Chem. Mater. 13 (2001)733-737.

[11] C.-H. Li, Z.-X. Yu, K.-F. Yao, S.-F. Ji, J. Liang, Nitrobenzene hydrogenation with carbon nanotube-supported platinum catalyst under mild conditions, J. Mol. Catal. A: Chem. 226 (2005) 101-105.

[12] G. Vijayaraghavan, K. J. Stevenson, Synergistic assembly of dendrimer-templated platinum catalysts on nitrogen-doped carbon nanotube electrodes for oxygen reduction, Langmuir 23 **(**2007) 5279-5282.

[13] A.L. Linsebigler, G. Lu, J.T. Yates, Photocatalysis on TiO_2 surfaces: principles, mechanisms, and selected results, Chem. Rev. 95 **(**1995) 735-758.

[14] C. C. Yang, S. J. Chiu, W. C. Chien, Development of alkaline direct methanol fuel cells based on cross linked PVA polymer membranes, J. Power Sources 162 **(**2006) 21-29.

[15] K.-M. Choi, T. Akita, T. Mizugaki, K. Ebitan, K. Kaneda, Highly selective oxidation of allylic alcohols catalysed by monodispersed 8-shell Pd nanoclusters in the presence of molecular oxygen, New J. Chem. 27 **(**2003) 324-328.

[16] J. M. Macak, H. Tsuchiya, A. Ghicov, K. Yasuda, R. Hahn, S. Bauer, P. Schmuki, TiO_2 nanotubes: self-organized electrochemical formation, properties and applications, Curr. Opin. Solid State Mater. Sci. 11 (2007) 3-18.

[17] K. Lee, A. Mazare, P.Schmuki, One-dimensional titanium dioxide nanomaterials: nanotubes, Chem. Rev. 114 **(**2014) 9385-9454.

[18] J. M. Macak, M. Zlamal, J. Krysa, P. Schmuki, Self-organized TiO_2 nanotube layers as highly efficient photocatalysts, Small 3 (2007) 300-304.

[19] I. Paramasivam, H. Jha, N. Liu, P.Schmuki, A Review of photocatalysis using self-organized TiO_2 nanotubes and other ordered oxide nanostructures, small 8 **(**2012) 3073-3103.

[20] V. C. Anitha, A. N. Banerjee, G. R. Dillip, S. W. Joo, B.K. Min, Nonstoichiometry-induced enhancement of electrochemical capacitance in anodic TiO_2 nanotubes with controlled pore diameter, J. Phys. Chem. C 120 **(**2016) 9569-9568.

[21] Z.D. Gao, X. Zhu, Y.H. Li, X. Zhou, Y.Y Song, P.Schmuki, Carbon cladded TiO_2 nanotubes: fabrication and use in 3D-RuO_2 based supercapacitors, Chem Commun. 36 **(**2015) 7614-7617.

[22] H. Mirabolghasemi, N. Liu, K. Lee, P. Schmuki, Formation of 'single walled' TiO_2 nanotubes with significantly enhanced electronic properties for higher efficiency dye-sensitized solar cells, Chem. Commun. 49 (2013) 2067-2069.

[23] X.Gao, J. Li, J. Baker, Y. Hou, D. Guan, J. Chen, C. Yuan, Enhanced photovoltaic performance of perovskite $CH_3NH_3PbI_3$ solar cells with freestanding TiO_2 nanotube array films, Chem. Commun. 50 **(**2014) 6368-6371.

[24] J. M.Macak, T. Kohoutek, L.Wang, R. Beranek, Fast and robust infiltration of functional material inside titania nanotube layers: case study of a chalcogenide glass sensitizer, Nanoscale 5 **(**2013) 9541-9545.

[25] M. Krbal, J. Prikryl, R. Zazpe, H. Sopha, J. M. Macak, CdS-coated TiO_2 nanotube layers: downscaling tube diameter towards efficient heterostructured photoelectrochemical conversion, Nanoscale, 9 (2017) 7755-7759.

[26] M. Krbal, H. Sopha, V. Podzemna, S.Das, J.Prikryl, J.M. Macak, TiO_2 nanotube/chalcogenide-based photoelectrochemical Cell: nanotube diameter dependence study, J. Phys. Chem. C. 121 (2017) 6065-6071.

[27] K. Gulati, S. Ramakrishnan, M.S. Aw, G.J. Atkins, D.M. Findlay, D. Losic, Biocompatible polymer coating of titania nanotube arrays for improved drug elution and osteoblast adhesion, Acta Biomater, 8 (2012) 449-456.

[28] M. Kulkarni, A.Mazare, E. Gongadze, S. Perutkova, V. Kralj- Iglic, I. Milosev, P.Schmuki, A. Iglic, M. Mozetic, Titanium nanostructures for biomedical applications, Nanotechnology, 26 (2014) 062002 (18pp).

[29] N. K. Shrestha, J.M. Macak, F. Schmidt-Stein, R. Hahn, C. T. Mierke, B. Fabry, P. Schmuki, Magnetically guided titania nanotubes for site-selective photocatalysis and drug release, Angew. Chem. Int. Ed. 48 (2009) 969-972.

[30] V. C. Anitha, J.-H. Lee, J. Lee, A. N. Banerjee, S .W. Joo, K.B. Min, Biofilm formation on a TiO_2 nanotube with controlled pore diameter and surface wettability, Nanotechnology, 26 **(**2015) 065102 (10pp).

[31] H. Inoue, T. Abe, C. Iwakura, Successive hydrogenation of styrene at a palladium sheet electrode combined with electrochemical supply of hydrogen, Chem. Commun. 1996, 55-56.

[32] Y. C. Tan, N. H. H. Abu Bakar, W. L. Tan, M. A. Bakar, ICIR Euroinvent. IOP Conf. Series: Materials Science and Engineering 133 **(**2016) 012017 (10pp).

[33] C. Smit, M. W. Fraaije, A. J. Minnaard, Reduction of carbon-carbon double bonds using organocatalytically generated diimide, J. Org. Chem. 73 (2008) 9482-9485.

[34] J. G. de Vries, C. J. Elsevier, Handbook of homogeneous hydrogenations, Wiley-VCH Verlag GmbH & Co. KGaA, Weinheim, New York, 2007.

[35] J. Li, B. Zhang, Y. Chen, J. Zhang, H. Yang, J. Zhang, X. Lu, G. Li, Y. Qin, Styrene hydrogenation performance of Pt nanoparticles with controlled size prepared by atomic layer deposition, Catal. Sci. Technol. 5 **(**2015) 4218-4223.

[36] J. Mondal, K. T. Nguyen, A. Jana, K. Kurniawan, P. Borah, Y. Zhao, A. Bhaumik, Efficient alkene hydrogenation over a magnetically recoverable and recyclable Fe_3O_4@GO nanocatalyst using hydrazine hydrate as the hydrogen source, Chem. Commun. 50 **(**2014) 12095-12097.

[37] R. V. Jagadeesh, G. Wienhofer, F. A. Westerhaus, A. E. Surkus, H. Junge, K. Junge, M. A. Beller, A Convenient and general ruthenium-catalyzed transfer hydrogenation of nitro- and azobenzenes, Chem. Eur. J. 17 (2011) 14375-14379.

[38] S. Horn, C. Gandolfi, M. Albrecht, Transfer hydrogenation of ketones and activated olefins using chelating NHC ruthenium complexes, Eur. J. Inorg. Chem. 2011(2011) 2863-2868.

[39] S. Gladiali, E. Alberico, Asymmetric transfer hydrogenation: chiral ligands and applications, Chem. Soc. Rev. 35 (2006) 226-236.

[40] P. S. Kumbhar, J. Sanchez-Valente, J. M. M. Millet, F. Figueras, Mg–Fe hydrotalcite as a catalyst for the reduction of aromatic nitro compounds with hydrazine hydrate, J. Catal. 191(2000) 467-473.

[41] S. M. Auer, J. D. Grunwaldt, R. A. Koppel, A. Baiker, Reduction of 4-nitrotoluene over Fe-Mg-Al lameller double hydroxides, J. Mol. Catal. A.Chem. 139 (1999) 305-313.

[42] R. Kadyrov, T. H. Riermeier, Highly enantioselective hydrogen-transfer reductive amination: catalytic asymmetric synthesis of primary amines, Angew. Chem. Int. Ed. 42 (2003) 5472-5474.

[43] A. Dhakshinamoorthy, S.Navalon, D.Sempere, M.Alvaro, H.Garcia, Reduction of alkenes catalyzed by copper nanoparticles supported on diamond nanoparticles, Chem. Commun. 49 **(**2013) 2359-2361.

[44] E. W. Schmidt, Hydrazine and Its Derivatives: Preparation, Properties, and Applications, Wiley & Sons, New York, 2nd ed., 2001, 2475 (2232pp).

[45] D. J. Pasto, R. T. Taylor, Reductions with Diimide, in Organic Reactions, ed. V. L. A. Paquette, Wiley & Sons, New York, 1991.

[46] U. Sharma, P. Kumar, N. Kumar, V. Kumar, B. Singh, Highly chemo- and regioselective reduction of aromatic nitro compounds catalyzed by recyclable copper(II) as well as cobalt(II) phthalocyanines, Adv. Synth. Catal. 352 **(**2010) 1834-1840.

[47] M. Benz, R. Prins, Kinetics of the reduction of aromatic nitro compounds with hydrazine hydrate in the presence of an iron oxide hydroxide catalyst, Appl. Catal., A. Gen 183 **(**1999) 325-333.

[48] M. Lauwiner, P. Rys, J. Wissmann, Reduction of aromatic nitro compounds with hydrazine hydrate in the presence of an iron oxide hydroxide catalyst. I. The reduction of monosubstituted nitrobenzenes with hydrazine hydrate in the presence of ferrihydrite, Appl. Catal., A. Gen 172 **(**1998) 141-148.

[49] P. G .Ren, D. X. Yan, X. Ji, T. Chen, Z. M. Li, Temperature dependence of graphene oxide reduced by hydrazine hydrate, Nanotechnology 22 (2011) 055705 (8pp).

[50] Y. J. Gao, D. Ma, C. L. Wang, J. Guan, X. H. Bao, Reduced graphene oxide as a catalyst for hydrogenation of nitrobenzene at room temperature, Chem. Commun. 47 (2011) 2432-2434.

[51] Y. Y. Song, Z. D. Gao, P. Schmuki, Highly uniform Pt nanoparticle decoration on TiO_2 nanotube arrays: a refreshable platform for methanol electrooxidation, Electrochem. Commun. 13((2011) 290-293.

[52] X. Pang, D. He, S. Luo, Q. Cai, An amperometric glucose biosensor fabricated with Pt nanoparticle-decorated carbon nanotubes/TiO_2 nanotube arrays composite, Sens. Actuators B Chem 137 (2009) 134-138.

[53] S. Mahshid, C. Li, S. S. Mahshid, M. Askari, A. Dolati, L. Yang, Q. Cai, Sensitive determination of dopamine in the presence of uric acid and ascorbic acid using TiO_2 nanotubes modified with Pd, Pt and Au nanoparticles, Analyst 136 (2011) 2322-2329.

[54] M. Tian, G. Wu, A. Chen, Unique electrochemical catalytic behavior of Pt nanoparticles deposited on TiO_2 nanotubes, ACS Catal. 2(2012) 425-432.

[55] L. Xing, J. Jia, Y. Wang, B. Zhang, S. Dong, Pt modified TiO_2 nanotubes electrode: preparation and electrocatalytic application for methanol oxidation, Int. J. Hydrog.Energy 35 (2010) 12169-12173.

[56] L. C. Almeida, M. V. Zanoni, Decoration of Ti/TiO_2 nanotubes with Pt nanoparticles for enhanced UV-Vis light absorption in photoelectrocatalytic process, J. Braz. Chem. Soc. 25 (2014) 579-588.

[57] H. Sopha, L. Hromadko, K. Nechvilova, J. M. Macak, Effect of electrolyte age and potential changes on the morphology of TiO_2 nanotubes, J. Electroanal. Chem. 759 **(**2015) 122-128.

[58] Z. Q. Tian, S. P. Jiang, Y. M. Liang, P. K. Shen, Synthesis and characterization of platinum catalysts on multiwalled carbon nanotubes by intermittent microwave irradiation for fuel cell applications, J. Phys. Chem. B. 110 (2006) 5343-5350.

[59] C. Dablemont, P. Lang, C. Mangeney, J.Y. Piquemal, V. Petkov, F. Herbst, G. Viau, FTIR and XPS study of Pt nanoparticle functionalization and interaction with alumina, Langmuir 24 (2008) 5832-5841.

[60] B. Erdem, R. A. Hunsicker, G. W. Simmons, E. D. Sudol, V. L. Dimonie, M. S. El-Aasser, XPS and FTIR surface characterization of TiO_2 particles used in polymer encapsulation, Langmuir 17 (2001) 2664-2669.

[61] P. Serp, B. Machado, Carbon (Nano) materials for catalysis, in nanostructured carbon materials for catalysis, 2015, 1-45.